Geopersia 2022, 12(1): 89-106
DOI: 10.22059/GEOPE.2021.324799.648618

RESEARCH PAPER

Impact of complex tectonics on the development of geo-pressured zones: A case study from petroliferous Sub-Himalayan Basin, Pakistan

Ali Wahid [1,*], Abdur Rauf [1], Syed Haroon Ali [2], JahanzebKhan [1], Muhammad Atif Iqbal [3], Abdul Haseeb [1]

[1] Institute of Geology, University of Azad Jammu and Kashmir, Pakistan
[2] Department of Earth Sciences, University of Sargodha, Sargodha, 40100, Pakistan
[3] Department of Petroleum Engineering, Curtin University, Australia

Received: 31 May 2021, Revised: 25 July 2021, Accepted: 26 August 2021

Abstract
In petroliferous basins, integration of regional and local tectonics along with well data is used to understand the generation of geo-pressured variations in different lithological units. In the last 40 years, abnormal geo-pressured zones is the main challenge during hydrocarbons drilling in the tectonically complex Kohat Sub-basin, Sub Himalayas. The trapped fluid in post-Eocene strata generated the over-pressure zones and triggered drilling problems. The present study is an integration of data, by use of regional maps, seismic lines, and formation pressure using Eaton's equation to understand the possible causes for the development of geo-pressured zones. Where, regional maps and seismic lines were employed for deciphering the regional and local tectonics, respectively. Porosity function and Normal Compaction Trend (NCT) curve were utilized for the identification of abnormal pore pressure zones (over-pressure and under-pressure zones). Three major stress regimes were interpreted. The results show that the mechanism of over-pressure zones developed as a combination of effective horizontal stresses, lithological variations and rapid sedimentation. The Normal Compaction Trend (NCT) line and porosity function indicated that the 1st and 2nd stress regime consists of major abnormal geo-pressured zones. Therefore, it is concluded that these stress regimes experienced more overburden pressure and fracture pressure. Consequently, it is suggested that the results of geo-pressure estimation from this work could be used for the appropriate mud weight during drilling in analogous tectonic settings..

Keywords: Tectonics, Abnormal Pore Pressure, Overburden Pressure, Fracture Pressure, Basin Analysis.

Introduction

The occurrence of overburden or over-pressure zones affects drilling success and reservoir depletion procedures (Leila et al., 2021; Radwan et al., 2020; Sen et al., 2020; Wang & Wang, 2015). There are many factors that generate abnormal geo-pressured zones in subsurface formations. The tectonic stresses can be one of the major causes of abnormal pore pressure development. Here, the horizontal stresses generate the tectonic forces and produce abnormal geo-pressured zones (Nwonodi & Dosunmu, 2021; Zhang et al., 2020; Brahma & Sircar, 2018; Huffman, 2002).

The seismic lines and wireline well log dataset can be used to determine the geo-pressured zones (Bashir et al., 2020, 2021a; Radwan et al., 2019; Haris et al., 2018; Mukerjiet et al., 2002).

* Corresponding author e-mail: ali.wahid@ajku.edu.pk

This research is based on the interpretation of regional and local faults in various stress regimes. Impact on geo-pressure development is interpreted by integrating regional maps and seismic sections. Here, the geo-pressure investigation includes the determination of pore pressure, overburden pressure and fracture pressure by using well logs. The pore pressure or formation pressure is the pressure of fluids present in the pores of the sedimentary rocks or any other rock matrix (Zhang et al., 2019; Mouchet & Mitchell, 1989). It is calculated widely by comparing the neutron, sonic, or resistivity responses of the logs (Bashir et al., 2021b; Gyllenhammar, 2020; Tingay et al., 2009). The normal pore pressure within the sedimentary rocks is called hydrostatic pressure. The Normal Compaction Trend (NCT) line and porosity function can be implemented to identify these abnormal geo-pressured zones (Radwan et al., 2019; Zhang, 2011). The NCT line is the linear trend response which is used to interpret the compaction disequilibrium with depth and is calculated from the sonic or density log (Velázquez-Cruz et al., 2017; Terzaghi, 1943). The scale and complexity of the NCT slope are greatly influenced by the structural settings (Radwan et al., 2019). However, the porosity of rocks greatly affects the pore pressure of fluids in the rock formations. When the rock has enough porosity to accumulate fluids, the pressure generated by effective stresses in the rock formation could be over-pressured (Eyinla et al., 2021; Baouche et al., 2020; Zhang, 2011). The abnormal geo-pressure results in the higher or lower pore pressure than the normal hydrostatic pressure. The upper boundary of abnormal pore pressure is the fracture pressure and is equivalent to the minimum horizontal stress (Zhang, 2011).

Previously, in Pakistan, the geo-pressure investigation was concerned with the extent and over-pressuring during drilling in Potwar Basin (Khan, 2017; Law et al., 1998; Kadri, 1991). These investigations revealed that tectonic compression and compaction disequilibrium were the reasons for the geo-pressure generation (Khan, 2017). However, the integration of tectonics and well data was missing for Kohat Basin. The Kohat Sub-basin is part of the Upper Indus Basin of Pakistan. It is structurally complex and most of the hydrocarbons are produced from the structurally trapped reservoirs (Wasim, 2004; Zaidi et al., 2013; Yasin et al., 2021). The area contains both the carbonates and clastic proven hydrocarbon reservoirs (Ali, 2009a; Khalid et al., 2012). The basin is highly over-pressured due to compressional tectonics. Abnormal geo-pressure is the major issue related to drilling (Law et al., 1998; Wahid et al., 2016).

It is difficult to drill these reservoirs as the abnormal geo-pressured zones were encountered in the post-Eocene rocks (Khan, 2017; Law et al., 1998). Due to this problem, the drilling of wells remained a difficult task and involved high drilling costs (Erge et al., 2020). The petroleum industry needs to assess the abnormal geo-pressured zones before drilling the hydrocarbon reservoirs. Moreover, it could help to overcome the drilling problems like kicks, blowouts and mud losses (Abdali et al., 2021).

Hence, a detailed study on the geological impact including the tectonic and effective stresses for the generation of abnormal geo-pressure in the Kohat Sub-basin was needed. Therefore, this study will help to investigate and identify the major compressive stresses. The overburden pressure, fracture pressure and abnormal pore pressure which are responsible for the generation of geo-pressured zones in the study area. The formations that experienced the fracture pressure are assumed to be having tensile failure (Zhang, 2011). The hydrostatic pressure exceeds the shear strength of the formation, it will start cracking and results in mud loss during drilling. This geo-pressure investigation will be helpful in wellbore stability and drill pipe stuck issues by determining pore pressure and fracture gradient in the area of interest.

The aims of this paper are the following:

1. To delineate the rule of regional and local tectonics by regional maps and seismic data.
2. To identify the abnormal pore pressure zones (over-pressure and under-pressure zones) using the porosity function and NCT curve.
3. To measure quantitative abnormal pore pressure zones using Eaton's equation.

Geological Setting

Geologically, the Kohat Sub-basin is bounded by the Salt Range Thrust (SRT)/Trans-Indus Range to south, Main Boundary Thrust (MBT) to north, dextral strike-slip Kalabagh Fault (KF) to the east and Kurram-Parachinar Range to the west (Ali et al.,2021; Ghazi et al.,2020; Yasin et al.,2020; Ghazi et al.,2015; Ali, 2009a). Due to the Indian-Eurasian plate collision, the Himalayan mountain belt was formed and this area became extensively deformed (Ahmed et al., 2020, Yasin et al., 2020; Ali, 2009b). This deformation was due to the horizontal stresses acting from south and north because of the Indian and Eurasian plates movement, respectively (Baig and Lawrence, 1987). It is assumed that these major stress regimes in sedimentary sequences of the Kohat Sub-basin are responsible for the generation of abnormal geo-pressured zones. The area of interest is comprised of different formations from Permian up to recent age. In which, post-Eocene, Murree Formation and Kamlial Formation (Rawalpindi Group) were deposited in Miocene (Abbasii and Khan, 1990). The Chinji Formation, Nagri Formation and Dhok Pathan Formation are of Pliocene. The Quaternary Alluvium was deposited during the Pleistocene (Shah, 2009). Particularly, the abnormal geo-pressured zones are encountered at the post-Eocene Rawalpindi group and Siwaliks (Javed et al., 2021; Kadri, 1991) in the region. These formations consist of conglomerate, sandstone, siltstone and shale deposits in fluvial environments, in response to the southward advancing Himalayan thrusting (Law et al., 1998). As a result of the collision, the three distinct stress regimes (Fig. 1) have evolved in the Himalayan foreland fold and thrust belt (Ahmed et al., 2020; Law et al., 1998). The 1st stress regime was the time of the pre-collision of the Eurasian and Indian plates. The Eocene (50 mya) was considered as the geological time for the development of this stress regime. During this time the Indian plate moved towards the north and the Main Mantle Thrust was developed (Treloar et al., 1989). The early Miocene (13 mya) was the 2nd stress regime that formed the Main Boundary Thrust in the region (Zeitler et al., 1981). Due to this stress regime, the tectonic deformation was shifted to the Main Boundary Thrust in the south. The Pliocene (0.5 mya) is considered as the time of 3rd stress regime generation. During this time the early Pleistocene formations were thrust and exposed on the surface (Lisa et al., 2004).

Based on the literature, it is assumed that the area of interest is highly disturbed in terms of tectonics. The thrust faults are exposed at the surface. To comprehend the major subsurface faults, the surface map of the study area was generated (After Meissner et al., 1970). The following thrust faults, namely Dartapi Fault (DTF), Krapa Fault (KF), Muslimabad Fault (MAF), Nandraki Fault (NRF), Shakardara Fault (SF), Braghzbada Fault (BBF), Bab-e-Shakardara (BSF), Nari Banda Faults (NBF), Tola Bangi Khel Fault (TBTKF) and Chorlaki Fault (CF) were digitized (Fig. 2).

Materials and methods

The research is based on two wells namely, Chanda Deep-01 and Chanda-02, which are situated at Chanda Oil Field, eastern Kohat Sub-basin (Fig. 1). To determine the tectonics impact on the development of geo-pressure, the regional and local tectonics were studied by integrating regional maps (modified after Meissner et al., 1974) and seismic sections (Fig. 2). About six 2D seismic lines (Fig. 2), dipping towards the north were interpreted for the investigation of local tectonics. The interpretation of the dipping seismic lines helped to interpret the type of faults and their trends in the subsurface. The maximum and minimum horizontal and vertical stresses were also calculated by using the equation (2) and equation (6). These calculations were utilized to find major effective stresses and their influence on the generation of compressional tectonics in the region. The pressure induced by the overburden of rocks vertically is determined by using equation (1).

$S_{ev} = \rho_b$ x Depth x 0.433 (Opara et al., 2018) (1)

Where, S_{ev} = Vertical stress, D = Depth, 0.433 = Conversion factor from g/cm^3 to psi/ft, ρ_b= the bulk density directly taken from density log.

To find out the horizontal stresses, the Poisson's ratio, shear wave and compressional wave velocities were calculated. The horizontal stresses (S_{eh}) at any depth were calculated (Paul et al., 2010) by using equation (2). Whereas, equation (3), equation (4), and equation (5) were used to calculate the Poisson's ratio (Karakan, 2009; Gatenset al., 1990) and shear and compressional wave velocities (Greenberg and Castagna, 1992), respectively.

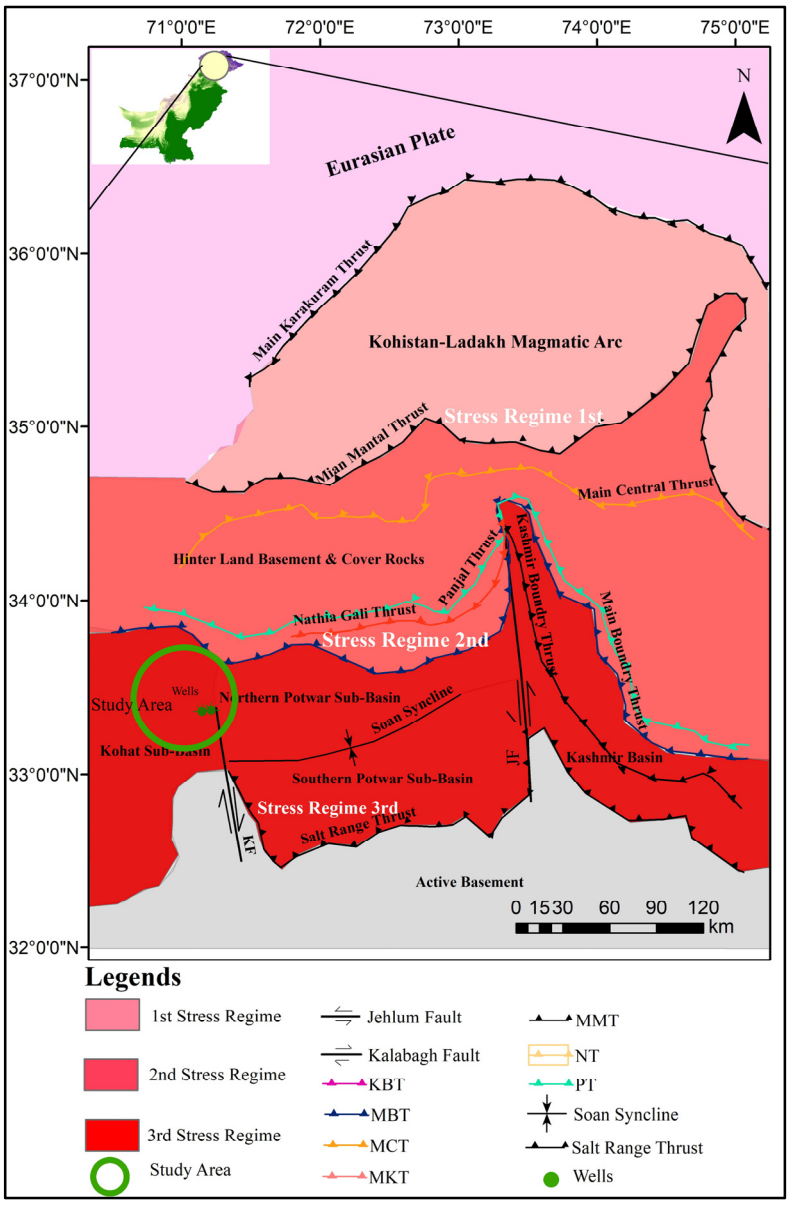

Figure 1. The regional tectonics map of northern Pakistan. The green circle shows the study area which is located in Kohat Sub-basin NNW of the dextral Kalabagh Fault. The study area is bounded by Main Boundary Thrust to north and west, The Kalabagh fault (dextral strike-slip fault) is in the east which runs north-south and the Surghar Range to the south. The 1st stress regime showing by light pink color, 2nd stress regime showing by dark pink color and 3rd stress regime showing by red color. It is assumed that the major stresses acting on the study area are majorly due to the 3rd stress regime. (Modified after Lisa et al., 2004; Baig& Lawrence 1987)

$(S_{eh}) = [(\gamma / (1 - \gamma)] * S_{ev}$ (2)

$\gamma = (1/2(V_p/V_s)*2-1)/ ((V_p/V_s)*2-1)$ (3)

V_s (km/s) = $(0.77*V_p-0.867)$ (4)

V_p (km/s) = $((10\text{^}3)/ (\Delta T *3.28))$ (5)

Where, S_{eh}= Horizontal Stress, γ= Poisson's ratio, S_{ev}= Vertical stresses, V_p= Compressional wave velocity, V_s= Shear wave velocity, and ΔT= sonic log.

The effective vertical stresses were calculated (Zhang, 2013; Terzaghi et al., 1996; Terzaghi, 1943) by using equation (6) in the study area.

$S_{Veff} = S_{ev} - PP$ (6)

Where, S_{Veff}= effective Vertical stresses, S_{ev}= Vertical stresses (Overburden stresses), PP= Pore pressure.

The vertical effective stresses are the difference between the overburden and pore pressure. Therefore, the assessed effective stress is also used for the pore pressure generation profile in the study area. The Normal Compaction Trend (NCT) line and porosity function were used for the identification of over-pressure zones (Zhang, 2013; Zhang, 2011). The NCT line was generated by using Eaton's sonic transit time for the over-pressure zones investigation. The zones where the transit time is high and experienced more compaction. The NCT line remains hydrostatic until the abnormal pore pressure influences the line. The Zhang (2011), equation (7) was used to find out the NCT line by using the sonic log.

$\Delta t_n = \Delta t_m + (\Delta t_{\text{mud line}} - \Delta t_{\text{matrix}})\, e^{-cd}$ (7)

Where, Δt_n= Sonic transit time (µs/ft) at the depth of interest, $\Delta t_{\text{mud line}}$= Transit Time (150 µs/ft) in Mudline, Δt_{matrix}= Transit Time (70 µs/ft) in Shale matrix, C= Compaction constant (0.0003 for sandstone, 0.0005 for shale, 0.0006 for limestone and 0.0004 for dolomite).

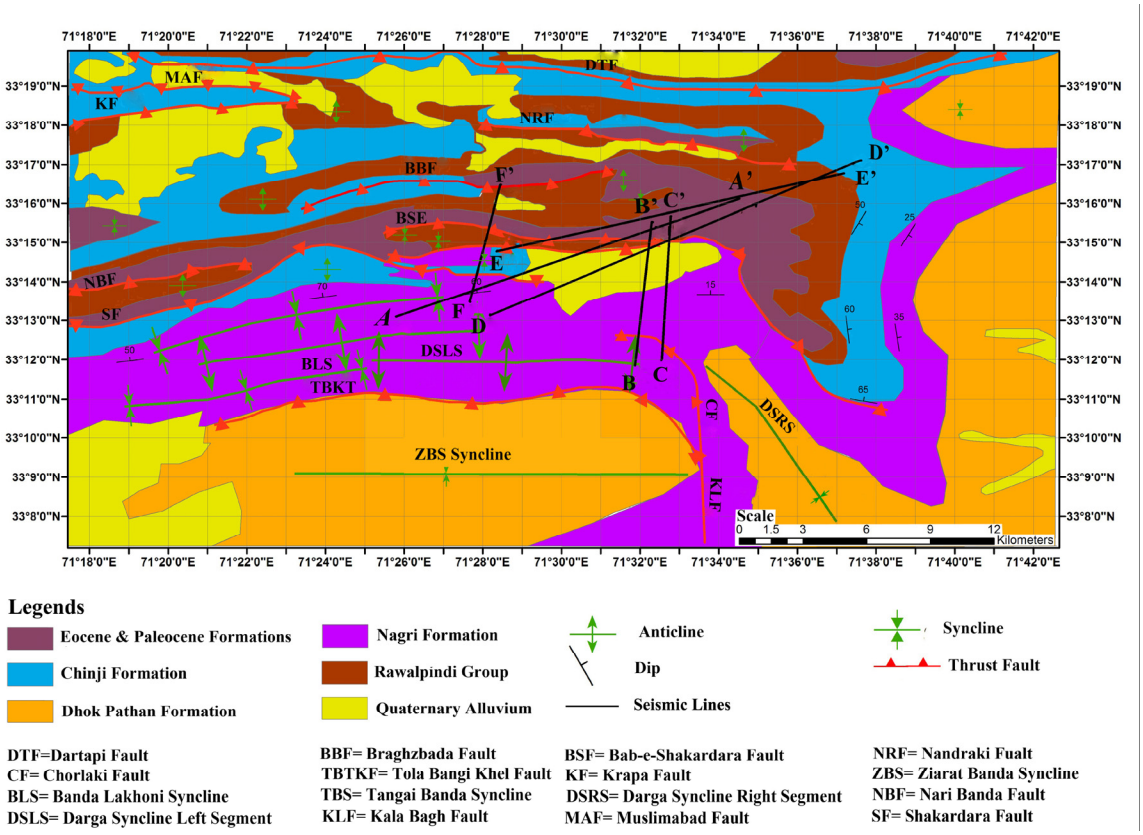

Figure 2. The surface tectonics and structural map of the study area (Kohat Sub-basin) having major and minor thrust and back thrust faults with repeated anticlines and synclines (Modified after Meissner et al., 1974)

The NCT line was generated based on lithological distributions of different zones. For this purpose, equation (8) and equation (9) was used to measure the gamma-ray index (Wahid et al., 2016; Salim et al., 2015) and shale volume respectively.

$I_{GR} = (GR_{recorded} - Gr_{clean}) / (GRshale - Gr_{clean})$ (8)

$V_{shale} = (I_{GR} / 3.00\text{-}2.00 \times I_{GR})$ (9)

Where, I_{GR} = Gamma-ray log Index, $GR_{recorded}$ = Reading of gamma-ray log at zone of interest, GR_{clean} = Carbonates or sandstone zone reading of GR log, GR_{shale} = Shale zone reading of GR log. V_{Shale}= Shale volume.

For the porosity estimation, equation (10) was used to find the sonic porosity (Yu *et al.,* 2018; Wyllie et al., 1958), whereas, equation (11) was used to calculate the density porosity (Wahid et al., 2016; Hilchie, 1978) of available well logs. Both porosities were integrated to estimate the average porosity by using the equation (12).

$\Delta\Phi_{sonic} = (\Delta T_{log}\text{-}\Delta T_{ma}) / (\Delta T_{fl} \text{-}\Delta T_{ma})$ (10)

$\rho_{\Phi} = (\rho_m\text{-}\rho_b (log)) / (\rho_m\text{-}\rho_f)$ (11)

$\Phi_{av} = \Phi_{\rho} + \Delta\Phi_{sonic} /2$ (12)

Hence, the intensities difference in the uncased borehole penetrated well were calculated by utilizing the density log recording gamma dispersion emitted from a source. The backscattering amount relied on a broad number of formations. The density log was not available in the upper part of the well so the equation (13) was used to extrapolate the density log into the upper intervals (Rana and Chandrashekhar, 2015).

$\rho_e = \rho_{ml} + A_0 (TVD - AG)\ \alpha$ (13)

Where, $_{\Phi av}$= Average porosity, Φ_{ρ} = Density Porosity, $\Delta\Phi_{sonic}$ = Sonic Porosity, ΔT = Sonic Travel Time in rock formation, ΔT_{ma} =Sonic Travel time in matrix, ΔT_{fl} = Sonic Travel Time in fluid, ρ_{Φ}= Density Porosity, ρ_m = Density of matrix, ρ_b= Bulk density derived from density log, ρ_f = Fluid density, ρ_e= Extrapolated density, ρ_{ml}= Normal ground level density (usually 2 gcc), AG= Air gap (Height of rig floor from ground), TVD= True Vertical Depth (ft), A_0 and α= Fitting parameters.

For the estimation of geo-pressured zones, the hydrostatic pressure, pore pressure, fracture gradient and overburden pressure curves were calculated. Equation (14) was used to generate the hydrostatic/normal pressure curve (Donaldson et al., 2002).

$\rho_h = \gamma_w * h$ (14)

Where ρ_h= hydrostatic pressure, γ_w= specific weight of water, h= height of a column of water.

The equation (15) from Eaton's sonic method (Eaton, 1975; Zhang, 2013) was used for the estimation of pore pressure in the study area.

$P_p = S_{ev} - (S_{ev} - \rho_h) (\Delta tn/\Delta t)\ X$ (15)

Where, P_p= Pore pressure, S_{ev}= Effective stresses, ρ_h= Hydrostatic pressure, Δtn= Sonic transit time (µs/ft) at particular zone, Δt= Sonic log reading from sonic log (µs/ft), X= Eaton's exponent.

The equation (16) from Eaton's sonic method (Zhang, 2013; Eaton, 1975) was used for the estimation of fracture gradient in the study area.

$FG = (\gamma / (1 - \gamma) * (S_{ev}\text{-}P_p) + P_p$ (16)

Where, FG=Fracture gradient, γ= Poisson's ratio, S_{ev} = Overburden pressure gradient, P_p= Pore pressure.

Results and Discussion

Regional Tectonic Setting

The regional tectonics was interpreted by digitizing the major and minor thrust and back thrust faults in the study area (Fig. 2). The DTF is the northward dipping thrust fault with ENE-WSW.

It plunges the Eocene rocks over the Late Miocene Chinji Formation. The Eocene rocks were thrusted over Kamlial Formation by a northward dipping KF thrust fault. This fault is located on the north-western side of the area of interest. The east to west trending MAF is the back-thrust fault and plunge the Jatta Gypsum above the Kamlial Formation. In the north, the east to west orientated NRF fault thrusts the Jatta Gypsum above the Kamlial Formation. In the central part of the study area, the SF fault is existing which trend towards the east to west and north to south. To the east of the area, this fault thrusts the Eocene rocks over the Nagri Formation, while the Kamlial Formation is on top of the Chinji Formation is in the middle. The BBF is an ENE–WSW-oriented thrust fault. It is a high-angle exposed fault on the surface and is in the middle of study area. An anticline exists in its west, in which the Chinji Formation is exposed towards the limb and Kamlial Formation in the core. The NBF and BSF are the splays of SF and developed in its north. These faults thrusted the Jatta Gypsum on top of the Kamlial Formation. The dextral strike-slip KLF is located in the south. The TBTK is the east to west trending fault present in the southwest and thrusted the Nagri Formation on top of the Dhok Pathan Formation. The KLF is orienting towards north to south and has a huge tectonic impact in the area (Fig. 2). It is present in the steeply dipping Nagri Formation. The CF and TBKF faults are kinematically linked with the KLF. The Banda Lakhoni Syncline is a plunging syncline having Nagri Formation in the core and Chinji Formation in the limbs. The Dhok Pathan Formation at the core and the Nagri Formation at the limbs of the Tangai Banda Syncline are exposed in the northeastern part of the area. In the Ziarat Banda Syncline, the Nagri Formation is in the limbs, whereas, the Dhok Pathan Formation is deposited in the core (Fig. 2). It is interpreted that the synclines and anticlines are present in the area of interest, in which the faults are cutting the anticline limbs due to compressional tectonics.

Tectonic and Effective Stress Analysis

The two seismic lines were interpreted in this paper to understand the tectonic conditions in the study area. For this purpose, the north-south oriented seismic dip line FF' was interpreted and a cross-section of the line was generated (Fig. 3C). In the subsurface, the Narai Banda Fault (NB) thrusted from the Palaeocene to Recent formations towards the north. The Palaeocene and Miocene rocks were interpreted towards the hanging wall, whereas, the Eocene and Kamlial Formations were deposited at the footwall. This fault is high angle dipping from south to north. The Shakardara Fault (SF) is cutting the seismic line FF' from the center, which thrusted the Palaeocene to Eocene rocks and further Eocene to Miocene rocks. It is dipping from north to south and cut the bottom in Cretaceous rocks, which is a low angle back thrust fault (Fig. 3C). The back-thrust fault thrusted the Permian rocks over Triassic and Triassic to the Jurassic rocks. The same low angle back thrust fault also runs parallel to Fault 1 which cuts the Shakardara Fault (SF) in Cretaceous rocks (Fig. 3C). The BSF fault is also a high angle thrust fault situated parallel to the BBF fault towards the southeast to northwest. These faults thrusted the strata upward from Jurassic to Pliocene. The Palaeocene Formations thrusted over the Miocene Formations including the Murree and Kamlial Formation as well as the Pliocene strata of Chinji and Nagri Formations. The thrusting of the formations to the northwest direction also takes place from Jurassic to Recent strata. The splays of the NBF cut the SF in Jurassic strata. The NBF thrust the Palaeocene rocks over the Pliocene rocks on the western side of the line FF'. Some of the other faults such as Chorlaki Fault (CF) and Tola Bandi Khel Fault (TBTKF) thrust, the formations below the Eocene in the northeast direction (Fig. 3C).Further, another seismic line CC' is also trending from north to south. The seismic line was directed across the strike of the major faults exposed on the surface (Fig. 2). In the north, the northward dipping Chorlaki Fault (CF) fault is the main thrust fault which dipped over the Cretaceous rocks and the Palaeocene rocks (Fig. 4C).

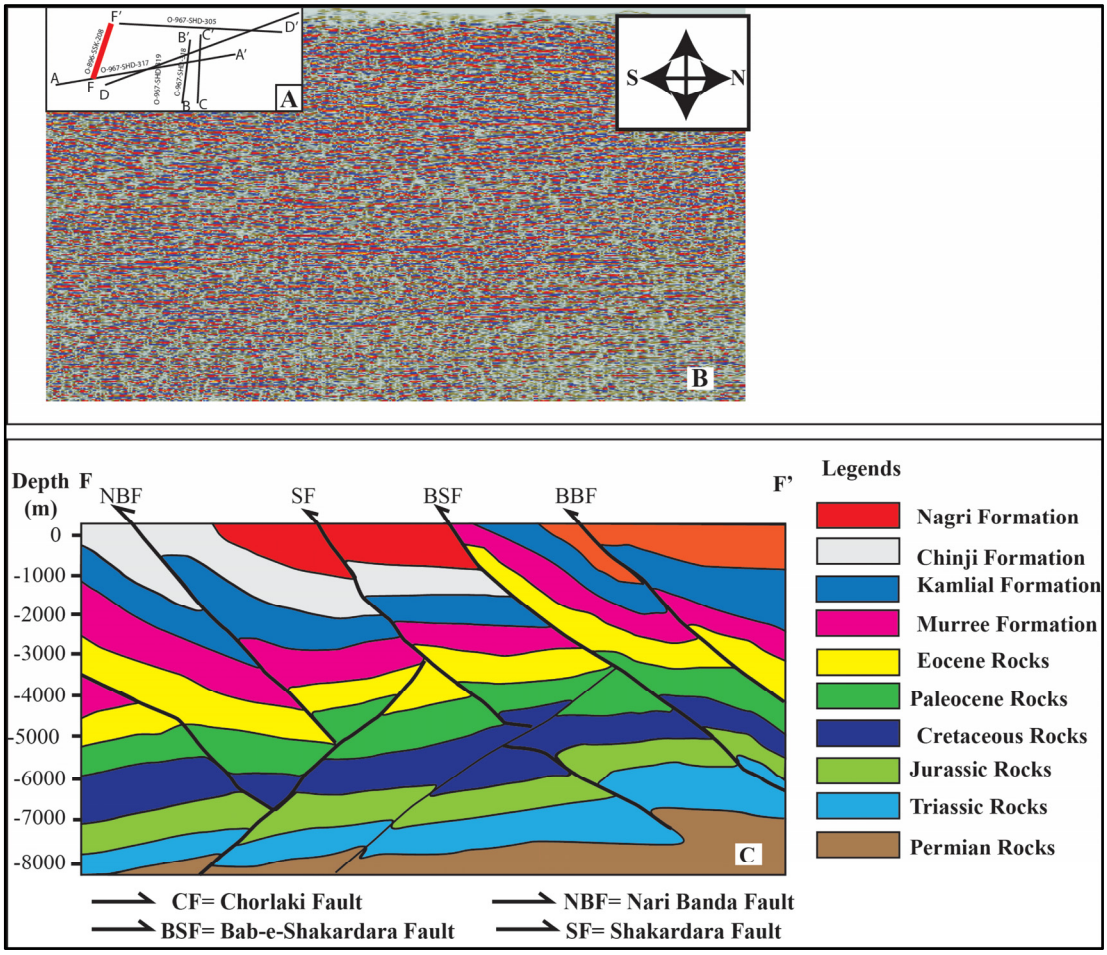

Figure 3. a) Base map of seismic lines,b) uninterested FF' seismic line,c) the cross-section of interpreted seismic line FF' having both thrust and back thrust faults. The Narai Banda Fault (NBF), Shakardara Fault), Dartapi Fault (DTF), Bab-e-Shakardara Fault (BSF) and Brazghbanda Fault (BBF) are dipping towards the north. The back thrust faults are dipping towards the north-south

The hanging wall formations (Palaeocene and Miocene) in the north were thrusted over the footwall strata towards the south, which consist of the Eocene and Kamlial Formation. The two subsurface parallel splay faults are also interpreted that were dipping towards the south. These back-thrust splays pushed the formations towards the north (Fig. 4C). The NBF thrust fault is present at the center of the seismic line CC' and dipping towards the north. On the southern side, the SF was dipping northward and thrusted the Cretaceous rocks over the Eocene rocks. Moreover, the Palaeocene rocks plunged over the Miocene rocks which further thrusted over the Chinji Formation. The Bab-e-Shakardara Fault (BSF) is a high-angle fault dipping northward and thrusted the Paleocene rocks over the Kamlial Formation (Fig. 4C).

The interpreted seismic lines showed that the area was extensively deformed having thrust and back thrust faults (Figs. 3 and 4). These deformations were due to compressive stresses propagated from north to south in response to the impact of the Eurasian and Indian plates (Fig. 1). The thrust faults were responsible for the uplifting and rapid sedimentation throughout the surface to the subsurface. Further, the rapid sedimentation due to sediment loading was also influenced by the non-gravitational impact due to compressional tectonics.

In this research, the effective horizontal and vertical stresses have been calculated based on three stress regimes that were developed due to major compressive forces acting on the region (Fig. 5). Hence, the previous literature helps to find that the study area consists of abnormal

geo-pressured zones (Khan, 2017; Law et al., 1998). Moreover, the seismic interpretation and the calculated effective horizontal and vertical stresses reveal that these stresses are responsible for the generation of abnormal geo-pressured zones. To keep this in mind, these stresses are considered as the major component in abnormal pore pressure generation in the area of interest. During the 1st stress regime (Triassic to Eocene, σ3), the impact of effective horizontal stresses was less than the effective vertical stresses (Fig. 5). This stress regime was responsible for the development of Main Mantle Thrust (MMT) in the region. The study area is away from the zone of MMT development (towards extreme north) which caused less impact of effective horizontal stresses than the effective vertical stresses (Fig. 1). Though, the 2nd stress regime (Miocene to Oligocene, σ2) and 3rd stress regime (Pleistocene to recent, σ1) experienced more effective horizontal stresses (Fig. 5) due to the development of MBT and SRT, respectively. It is interpreted that the 3rd stress regime caused the major impact on the generation of compressional stresses as this regime developed in the study area (Fig. 1).

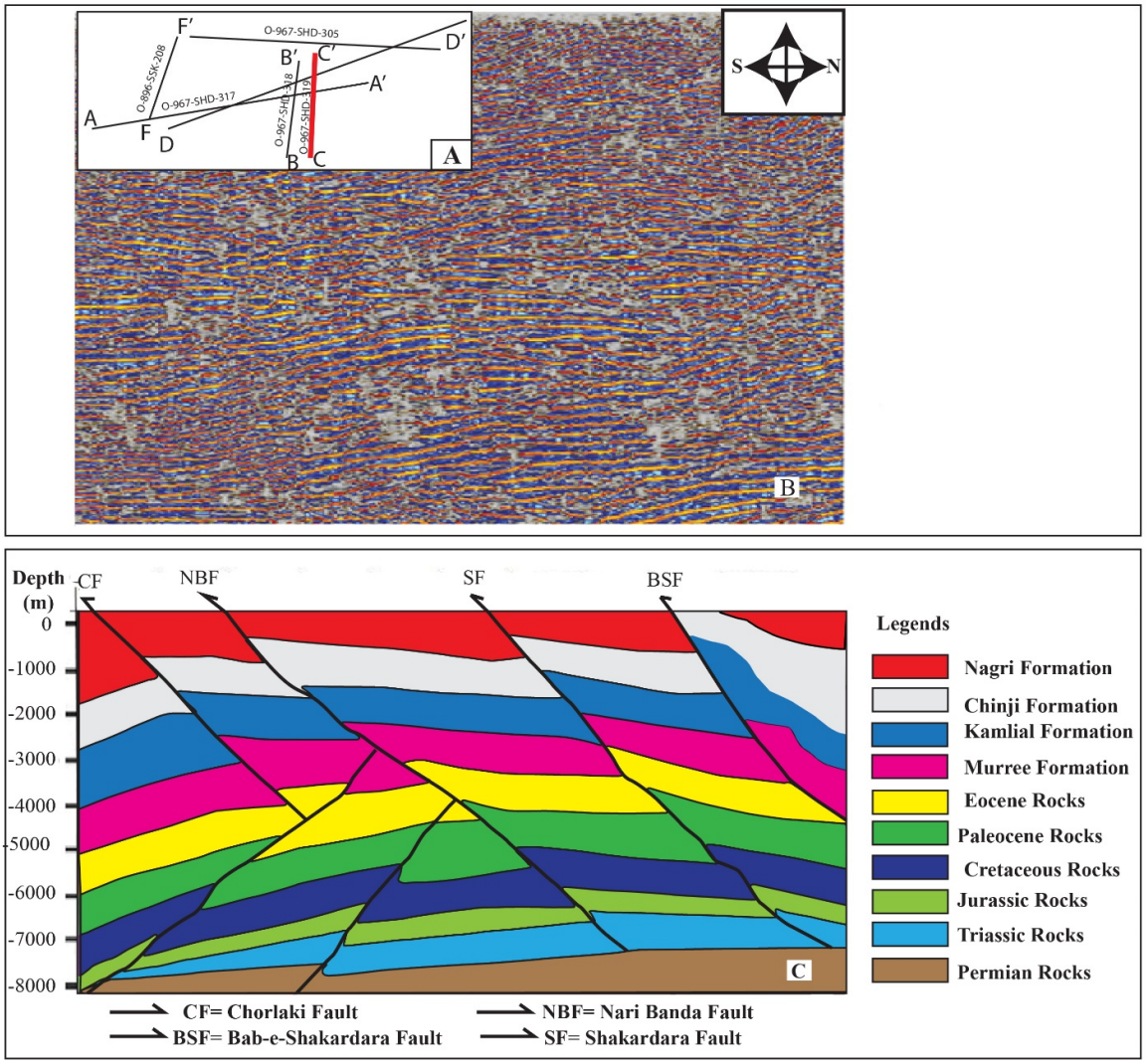

Figure 4. a) Base map of seismic lines, b) the uninterpreted CC'seismic line,c) the cross-section of CC' seismic line having thrust faults dipping toward the north to south. The Chorlakai Fault (CF), Narai Banda Fault (NBF), Shakardara Fault (SF), and Bab-e-Shakardara Fault (BSF) are the thrust faults whereas two back thrust faults are dipping southward

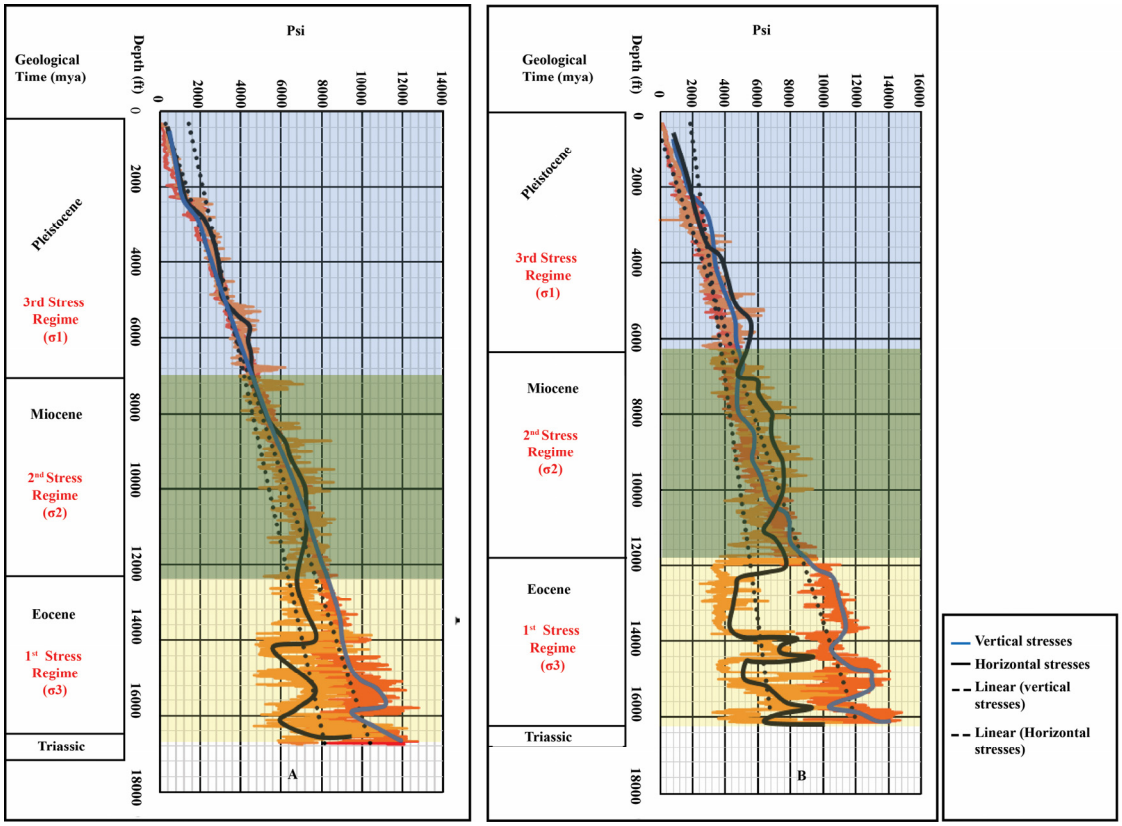

Figure 5. Effective vertical and horizontal stresses in a) Chanda Deep-01 and b) Chanda -02 well. The 1st stress regime (σ3) consists of high effective horizontal stresses than effective vertical stresses. The 2nd stress regime (σ2) and 3rd stress regime (σ1) experience more effective horizontal stresses due to the development of MBT and SRT respectively. The 3rd stress regime causes a major impact on the generation of compressional stresses as this regime is situated in the study area

Geo-Pressure Analysis

Abnormal Geo-Pressured Zones Identification

The physical features including the Normal Compaction Trend (NCT) line and the porosity function have been used for the abnormal geo-pressured zones identification. For this purpose, the NCT line was generated by using Eaton's sonic transit time (Fig. 6). Consequently, the zones where the transit time is high experienced more compaction in both the wells. The NCT line remained hydrostatic until the over or under-pressure zones influenced the line (Fig. 6). The deviation of the NCT line in the over-pressure zones indicated the development of the abnormal geo-pressure in the area. The top of the over-pressure zones has been identified from Miocene to Oligocene (2nd stress regime) and Triassic to Eocene (1st stress regime) in both the wells. Triassic to Eocene, the major abnormal geo-pressured zone was identified as this zone experienced high over-pressure due to overburden formations and compressional tectonics (Fig. 6). The Pleistocene age (1st stress regime) has undergone less development of abnormal pore pressure as it is near to the surface. The Chanda Deep-01 well has a top of under-compaction from 7500 ft., in contrast, the Chanda-02 well has a top under compaction below 6850 ft. depth. The top of over-pressure zones has been interpreted in different zones below this depth. In the 1st and 2nd stress regime, these abnormal pore pressure zones development were the result of effective horizontal stresses. These stresses increased the tectonic activities and may be responsible for the upward movement and trapping of fluid within the geological formations

and caused the abnormal pore pressure. Generally, the porosity of the geological formations decreases exponentially as it undergone more compaction from the surface towards depth. From Pleistocene to recent, the porosity is constantly decreasing up to the depth of 6900 ft. in Chanda Deep-01 well and 6400 ft. in Chanda-02 well (Fig. 7). The geo-pressure is considered to be hydrostatic up to this depth. Contrarily, the porosity reversals below these depths (in the 1st and 2nd stress regime) reflected the abnormal geo-pressured zones (Fig. 7). It is assumed that these regimes consist of porous zones that, were developed due to extreme tectonics and rapid sedimentation. These zones accumulated and trapped the fluid within the geological formations and caused the under-compaction.

Abnormal Geo-Pressure Estimation

The abnormal geo-pressured zones were estimated by generating overburden stress, pore pressure and fracture pressure curves. In this study, we correlated all the curves with the three tectonic regimes as discussed.

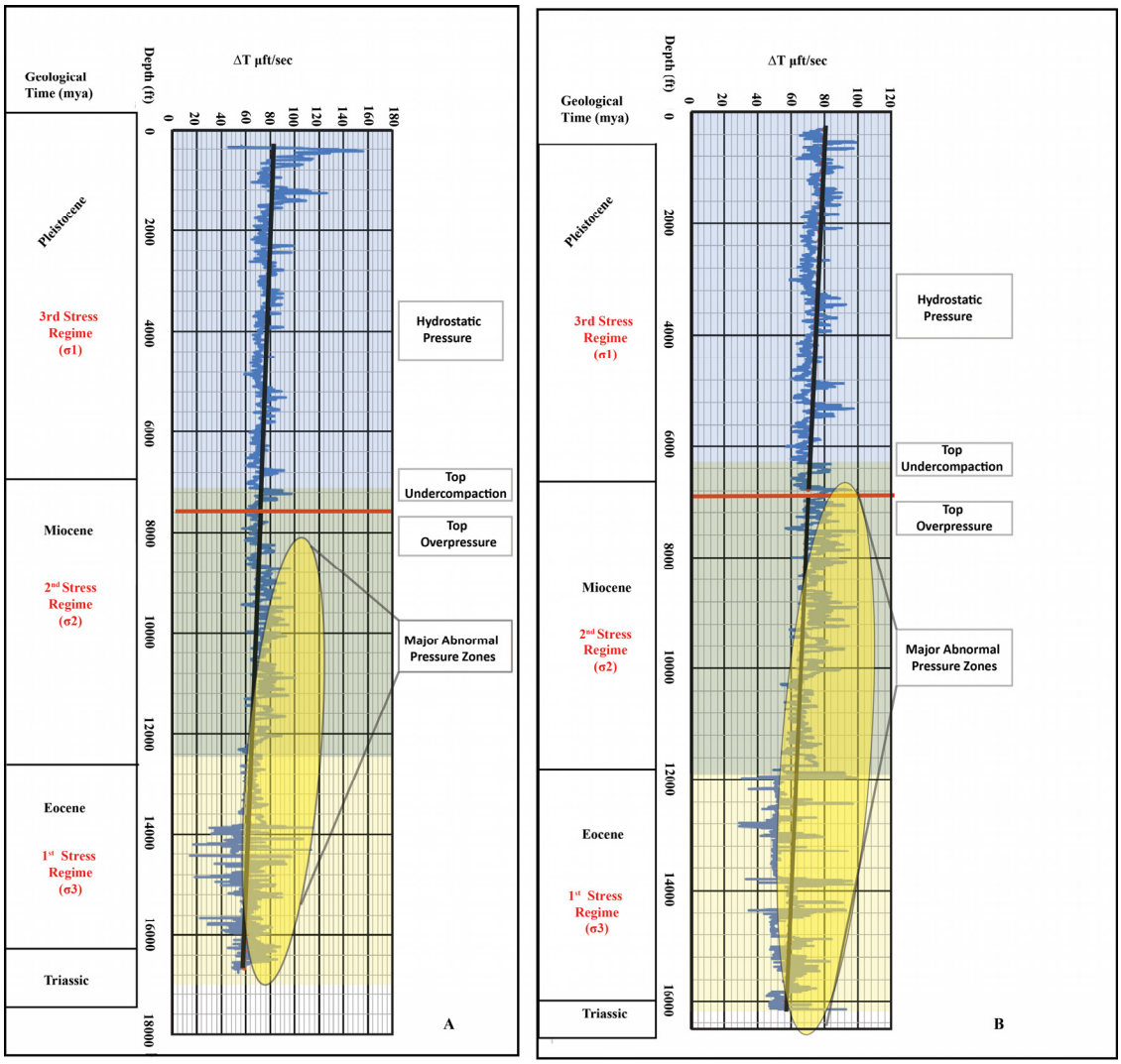

Figure 6. The NCT line a) in Chanda Deep-01 well, and b) in Chanda-02 well from sonic transit time for the major overpressure zones identification. The top of under-compaction zones is identified in 2nd stress regime to total depth in both the wells. The under-compaction and compressional tectonics are responsible for the generation of overpressure zones in the 2nd and 3rd stress regime

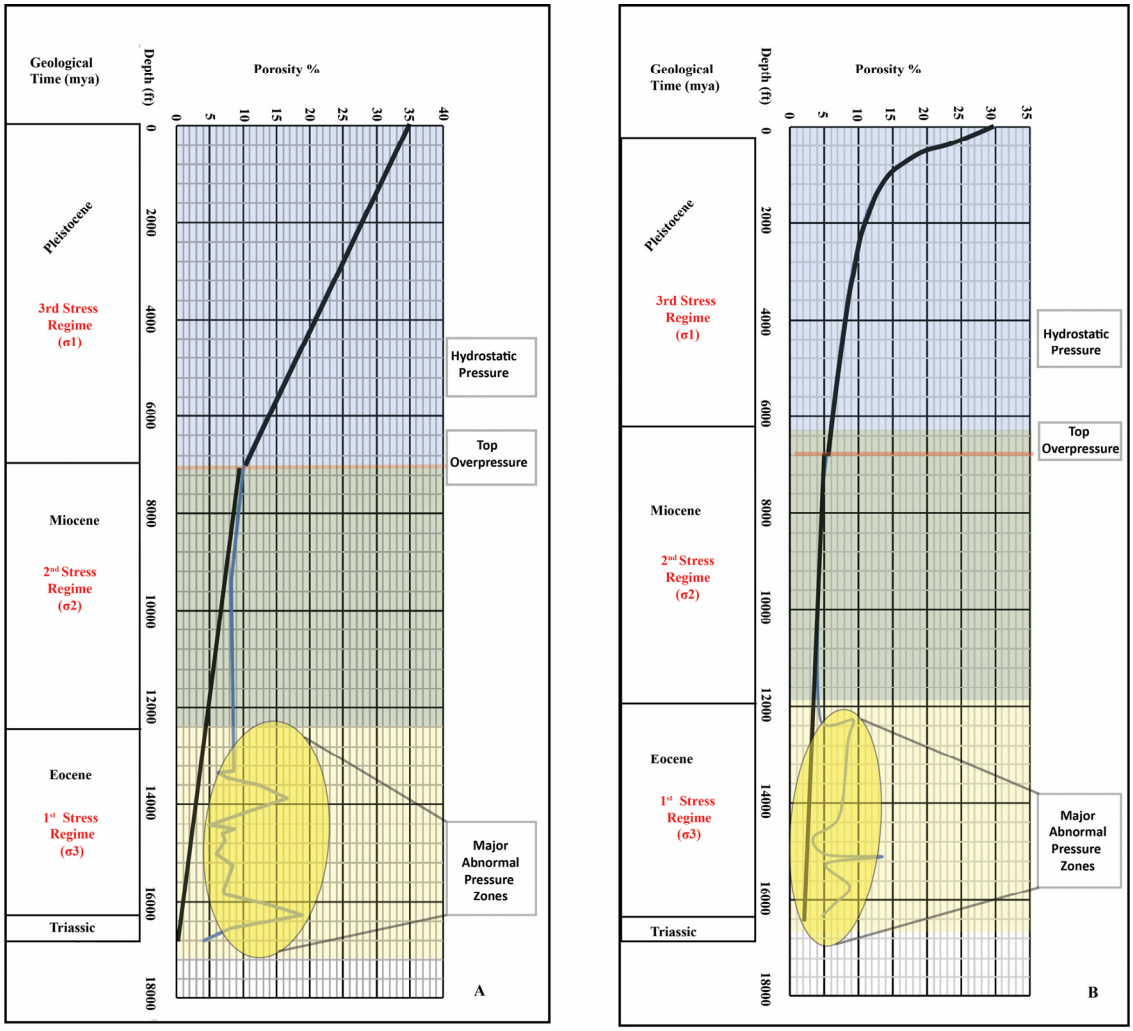

Figure 7. The porosity profile in a) Chanda Deep-1well and b) Chanda-02 well indicates the top of under-compaction zones in the 2nd stress regime up to total depth in both the wells. The profile indicates that the 1st stress regime consists of major abnormal pressure zones

The overburden pressure was calculated by extrapolating density values from both wells. Subsequently, it is the combination of pressure in the matrix and pores of the rocks, so the maximum overburden pressure was considered during the study. The overburden pressure is constantly increasing with depth in both wells (Fig. 8). However, during the 1st stress regime (Triassic to Eocene), the overburden pressure is fluctuating as these zones consist of the proven hydrocarbon zones. Which exert the opposite force against the horizontal overburden rocks and divert the effective vertical stresses. The maximum overburden pressure in this zone is 20217 psi with an average gradient of 1.11 in Chanda Deep-01 well. In contrast, it is 19770 psi with an average gradient of 1.14 in Chanda-02 well. In the 2nd stress regime, the maximum overburden pressure was 14815 psi and 13880 psi in both wells. Further, in the 3rd stress regime, the maximum calculated overburden pressure in both wells was estimated as 8122 psi and 7243 psi (Table 1). The overburden pressure was triggered majorly due to compressional stresses, thrust faulting and uplifting in the region. The calculated fracture pressure is indicated the rupture strength of different zones (Fig. 8). It is suggested that during the well drilling, the mud weight should be selected on the calculated values of the pore pressure and the fracture gradient. The mud weight higher than the fracture gradient results in the rupture of the rock formations and mud loss in the study area.

Table 1. The calculated overburden pressure, fracture pressure and abnormal pore pressure in three stress regimes by using Eaton Sonic method in Chanda Deep-01 and Chanda-02 well

Geological Age (Mya)	Chanda Deep-01						Chanda-02					
	Overburden Pressure (avg. psi)		Fracture Pressure (avg. psi)		Abnormal Pore pressure (avg. psi)		Overburden Pressure (avg. psi)		Fracture pressure (avg. psi)		Abnormal Pore pressure (avg. psi)	
	Max (psi)	Avg. G	Max (psi)	Avg .G	Max (psi)	Avg .G	Max (psi)	Avg . G	Max (psi)	Avg. G	Max (psi)	Avg. G
Triassic - Eocene	20217	1.11	12695	0.6	10310	0.5	19770	1.14	16341	0.73	10938	0.5
Early Miocene-Oligocene	14815	1.14	7936	0.6	9720	0.7	13880	1.15	11122	0.88	7937	0.6
Pleistocene -Recent	8122	1.04	4478	0.5	5528	0.69	7243	0.45	5591	0.7	3982	0.4

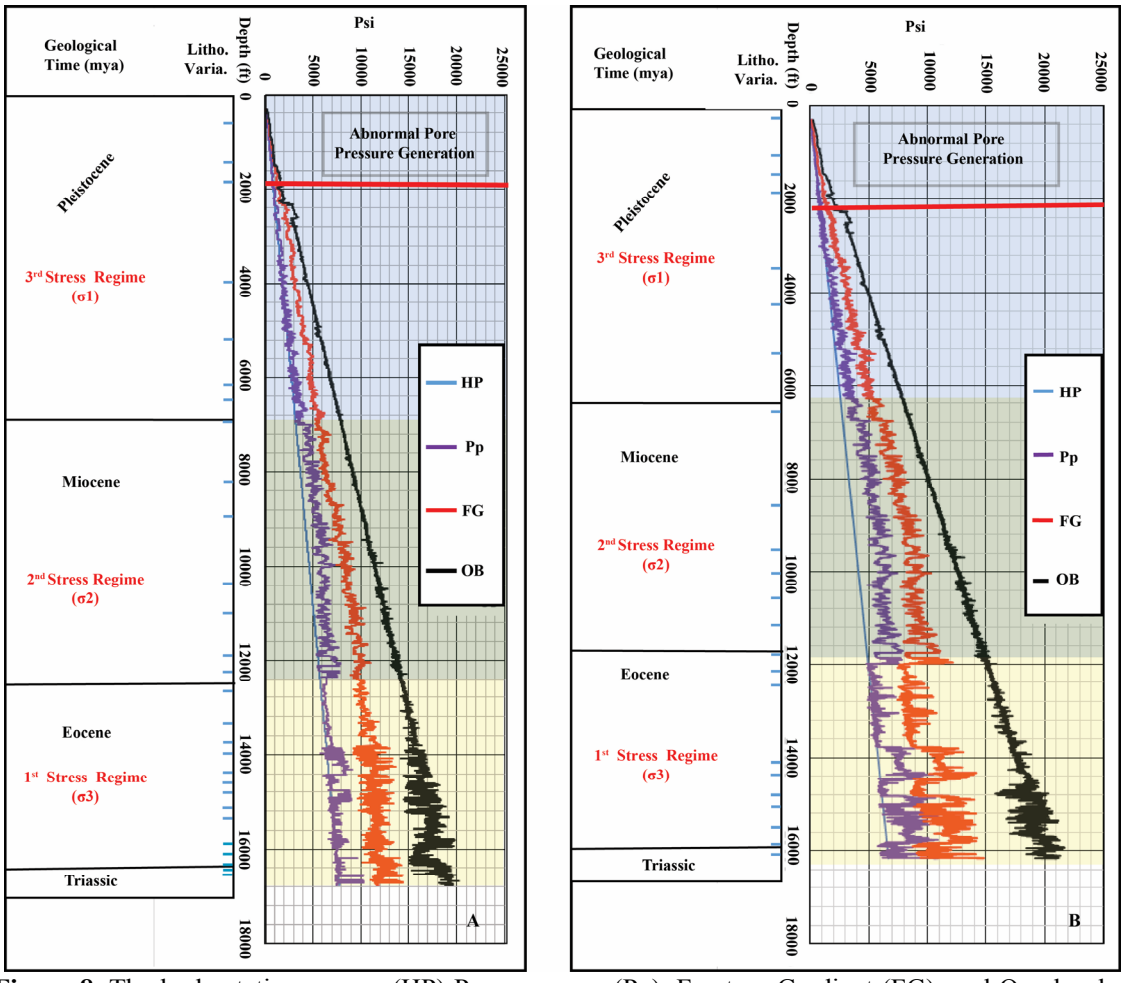

Figure 8. The hydrostatic pressure (HP) Pore pressure (Pp), Fracture Gradient (FG), and Overburden Pressure (OB) in a) Chanda Deep-1 and b) Chanda- 02 well. The abnormal geo-pressure generation is observed below 2000 ft. in both wells

The fracture gradient varied due to the change in lithologies, pore pressure and porosities. The 1st stress regime has major variations in lithologies due to which it experienced the fluctuating fracture gradient. This lithological variation is the indication of the rapid

sedimentation after the Indian-Eurasian plate collisions. The maximum fracture pressure in the 1st stress regime was 12695 psi (0.60 average fracture gradient) and 16341psi (0.73 average fracture gradient) in Chanda Deep-01 and Chanda-02 well, respectively. The maximum fracture pressure in the 2nd stress regime is 7936 psi (0.64 average fracture gradient) and 11122 psi (0.88 average fracture gradient). Conversely, the 3rd stress regime had maximum fracture pressure of 4478 psi (0.5 average fracture gradient) and 5591 psi (0.7 average fracture gradient). It is observed that the fracture pressure gradient is high in the 2nd stress regime (Table 1). This is due to the more compacted lithologies and has good thicknesses with no considerable variations during their deposition (Fig. 8).

Whereas, the abnormal pore pressure (high or low pore pressure) has been estimated from the near-surface, up to the depth of approximately 16000 ft on both the wells. The dominant abnormal geo-pressured zones have been identified in 1st and 2nd stress regimes, which were indicated from the extreme fluctuating pore pressure curve in these zones. The 1st stress regime has both the over and under-pressure zones. In the upper part of this regime, the hydrostatic pore pressure fluctuated below 14000 ft. depth. The maximum over pore pressure in this zone is 10310 psi and 10938 psi in Chanda Deep-01 and Chanda-02 well, correspondingly. The under-pressure zones in this regime also have the impact of extreme faulting.

The thrust faults due to tectonic impact may cause upward movement of trapped fluid within the geological formations through faults and lowered fluid pressure in 1st stress regime. Further, this regime consists of producing hydrocarbon reservoirs which might be another reason for under-pressure zones. While, the 2nd stress regime consists of Miocene Murree and Kamlial Formations which were deposited rapidly and trapped fluid in it and caused the abnormal over-pressure zones in the area. The increase in pore pressure values as compared to the hydrostatic pressure is the indication of the high-pressure zone in 2nd stress regime (Fig. 8). Moreover, the presence of fluid could be explained by the fact that the tectonic activity due to effective horizontal stresses charged the overlying formations. The reversal of the pressure regime could be attributed to the upward movement of fluid through thrust faults. As these fluids remain in the pore spaces of the formations are trapped and caused abnormal pore pressure zones with the increased overburden pressure. In contrast, the 3rd stress experienced abnormal pore pressure at depth of almost 2000 ft. in both wells due to the formation of Salt Range Thrust (SRT) fault in the region (Fig. 1). The calculated fracture pressure may be used with the pore pressure calculation to determine the safe range (upper limit) of mud weight during drilling.

The study helped to develop a relationship between different stress regimes and the impact of tectonics on the generation of geo-pressured zones in the study area. It is ascertained that the area has undergone through effective horizontal and vertical stresses. These stresses were responsible for the extreme tectonic activities in the region and one of the main components of the abnormal geo-pressure generation. It is suggested that while estimating the geo-pressure, the tectonic impact of its generation should be addressed. Further, the high-density drilling fluid and the increased mud weight should be used to control the abnormal geo-pressured zones in the study area. The calculated fracture pressure may be used with the pore pressure calculation to determine the safe range (upper limit) of mud weight during drilling. Moreover, the abnormal geo-pressured zones might be treated separately to seal these thief zones (overpressure zones) during drilling.

Conclusions

The following are the conclusions:

The interpreted seismic lines showed that the study area was extensively deformed having thrust and back thrust faults. This deformation is majorly caused by the effective horizontal stresses propagated from north to south, in response to the impact of the collision Eurasian-

Indian plates. Further, it originates the tectonic activity, uplifting, rapid rate of deposition and quick burial. The non-tectonic gravitational impact also caused rapid sedimentation as a result of sediment loading due to thrust faulting. With the help of seismic interpretation and calculated compressive stresses, it is concluded that the study area consists of abnormal geo-pressured zones from near-surface to the total depth.

The NCT line and porosity function also indicate the existence of abnormal geo-pressured zones, in which the 1st and 2nd stress regime consists of major effected zones.

The abnormal geo-pressured zones were indicated based on three different stress regimes acting in different geological times. It is interpreted that the overburden pressure is constantly increasing from the 3rd stress regime up to the 1st stress regime. Whereas, the fluctuation of the overburden pressure during the 1st stress regime is due to the presence of hydrocarbons/fluids, which generated the opposite force against the horizontal overburden formations. Though, the high geo-pressured zones in Miocene Murree and Kamlial Formations are due to trapped fluid in them.

The fluctuating fracture gradient during the 1st stress regime was due to rapid sedimentation, which results from the deposition of various lithological units from Triassic to Eocene. While, the 2nd and 3rd stress regimes consist of more compacted lithologies with no considerable variations during their deposition.

Overall, it is concluded that the 1st and 2nd stress regimes consist of dominant abnormal geo-pressure zones, which were indicated from the extreme fluctuating pore pressure curve in these zones. Moreover, the over-pressure zones developed in the 2nd stress regimes are due to trapped fluid and are considered as the major cause of severe drilling problems in the area. The 3rd stress experienced abnormal pore pressure majorly due to the formation of the Salt Range Thrust (SRT) fault in the region. It is recommended that the density of mud weight should be used according to the variations of the pore pressure and fracture pressure profile (Fig.8) with depth to maintain the wellbore stability in the future.

Acknowledgments

The authors are grateful to the Directorate General Petroleum Concession (DGPC) Islamabad, Pakistan for the provision of digital data. We thank Professor Dr. Ali Kananian (Editor-in-Chief, Geopersia), Prof. R. Dashti and another anonymous reviewer who provided critical helpful comments and suggestions to our manuscript; nevertheless, we take full responsibility for our interpretation.

References

Abbasii, I.A., Khan, M.A., 1990. Heavy mineral analysis of Molasse sediments, Trans-Indus Range, Kohat, Pakistan. Department Geol. Bull. Univ. Peshawar, 23: 215-229.

Abdali, M.R., Mohamadian, N., Ghorbani, H., Wood, D.A., 2021. Petroleum Well Blowouts as a Threat to Drilling Operation and Wellbore Sustainability: Causes, Prevention, Safety and Emergency Response. Journal of Construction Materials| Special Issue on Sustainable Petroleum Engineering ISSN, 2652, 3752.

Ahmed, N., Ali, S. H., Ahmad, M., Khalid, P., Ahmad, B., Akram, M. S., Din, Z. U., 2020. Subsurface structural investigation based on seismic data of the north-eastern Potwar basin, Pakistan.Indian Journal of Geo-Marine Sciences,49(7):1258-1268.

Ali, S. H., Shoukat, N., Bashir, Y., Qadri, S.M.T., Wahid, A., Iqbal, M.A., 2021. Lithofacies and Sedimentology of Baghanwala Formation (Early -Middle Cambrian), Eastern Salt Range, Pakistan, Pakistan Journal of Scientific and Industrial Research (PJSIR), (Accepted).

Ali, S.H., 2009a. Reservoir Characteristics of Early-Middle Cambrian Baghanwala Formation Eastern Salt Range Pakistan, SPE and PAPG Annual Technical Conference, Maximize Reserves - Optimize Exploitation, November 17-18, Serena Hotel, Islamabad (Abstract Book; 1-11).

Ali, S.H., 2009b.Lithostructural mapping of Ara-Basharat area Eastern Salt Range with special emphasize on bioturbations of the Kussak Formation and Reservoir Characteristics of the Baghanwala Formation, Eastern Salt Range, Pakistan. M.Sc. Thesis, University of the Punjab, Lahore.

Baig, M. S., Lawrence, R.D., 1987. Precambrian to Early Palaeozoic orogenesis in the Himalaya. Kashmir J. Geol, 5: 1-22.

Baouche, R., Sen, S., Sadaoui, M., Boutaleb, K., Ganguli, S. S., 2020. Characterization of pore pressure, fracture pressure, shear failure and its implications for drilling, wellbore stability and completion design-A case study from the Takouazet field, Illizi Basin, Algeria. Marine and Petroleum Geology, 120: 104510.

Bashir, Y., Faisal, M.A., Biswas, A., Abbas Babasafari, A., Ali, S.H., Imran, Q.S., Siddiqui, N.A., Ehsan, M., 2021a. Seismic expression of Miocene carbonate platform and reservoir characterization through geophysical approach: application in Central Luconia, offshore Malaysia. Journal of Petroleum Exploration and Production, 11(4): 1533-1544.

Bashir, Y., Babasafari, A.A., Alashloo, S.Y.M., Muztaza, N.M., Ali, S.H., Imran, Q.S., 2021b. Seismic wave propagation characteristics using conventional and advance modelling algorithm for d-data imaging. Journal of Seismic Exploration, 30(1): 21-44.

Bashir, Y., MohdMuztaza, N., MoussaviAlashloo, S.Y., Ali, S.H., Prasad Ghosh, D., 2020. Inspiration for Seismic Diffraction Modelling, Separation, and Velocity in Depth Imaging. Applied Sciences, 10(12): 4391.

Brahma, J., Sircar, A., 2018. Design of safe well on the top of Atharamura anticline, Tripura, India, on the basis of predicted pore pressure from seismic velocity data. Journal of Petroleum Exploration and Production Technology, 8(4): 1209-1224.

Dasgupta, T., Mukherjee, S., 2020. Global Overpressure Scenario. Sediment Compaction and Applications in Petroleum Geoscience. Advances in Oil and Gas Exploration & Production, 51-81.

Eaton, B. A., 1969. Fracture gradient prediction and its application in oil field operations. Journal of Petroleum Technology, 21(10)1: 1-353.

Eaton, B. A., 1975. The Equation for Geopressure Prediction from Well Logs. Society of Petroleum Engineers of AIME, Society of Petroleum Engineers, 5544.

Erge, O., Sakaoglu, K., Sonmez, A., Bagatir, G., Dogan, H.A., Ay, A. and Gucuyener, I.H., 2020. Overview and design principles of drilling fluids systems for geothermal Wells in Turkey. Geothermics, 88:101897.

Eyinla, D. S., Oladunjoye, M. A., Olayinka, A. I., Bate, B. B., 2021. Rock physics and geomechanical application in the interpretation of rock property trends for overpressure detection. Journal of Petroleum Exploration and Production, 11(1): 75-95.

Gatens, J. M., Harrison, C.W., Lancaster, D.E., Guidry, F.K., 1990. In-situ stress tests and acoustic logs determine mechanical properties and stress profiles in the Devonian shales. SPE Formation Evaluation, 5(03): 248-254.

Ghazi, S., Ali, S.H., Sahraeyan, M., Hanif, T., 2015. An overview of tectono-sedimentary framework of the Salt Range, northwestern Himalayan fold and thrust belt, Pakistan. Arabian Journal of Geosciences, 8(3): 1635-1651.

Ghazi, S., Ali, S.H., Shehzad. T., Ahmed, N., Khalid, P., Akram, S., Ali, S., Sami, J., (2020). Sedimentary, structural and Salt Range and its affects for the Potwar Province, Himalayan Geology, 41 (2): pp. 145-156.

Greenberg, M. L., Castagna J.P., 1992. Shear-wave estimation in porous rocks: Theoretical formulation, preliminary verification and applications. Geophysical Prospecting, 40 (2): 195-209.

Gyllenhammar, C. F., 2020. Why the resistivity log should not be used to calculate or predict pore pressure in the North Sea. First Break, 38(9): 57-63.

Haris, A., Murdianto, B. S., Sutattyo, R., Riyanto, A., 2018. Transforming seismic data into lateral sonic properties using artificial neural network: a case study of real data set. Chemical Engineering, 9(3).

Hilchie, D. W., 1978. Applied open hole log interpretation. Golden, Colorado, D.W. Hilchie, Inc, 1399:42-30.

Hubbert, M. K., Willis, D. G., 1957. Mechanics of hydraulic fracturing. Pet Trans AIME, 210: 153-68.

Huffman, A. R., 2002. The future of pore-pressure prediction using geophysical methods. The Leading Edge, 21(2): 199-205.

Javed, A., Wahid, A., Mughal, M.S., Khan, M.S., Qammar, R.S., Ali, S.H., Siddiqui, N.A., Iqbal, M.A.,

2021. Geological and Petrographic Investigations of the Miocene Molasse deposits in Sub-Himalayas, District Sudhnati, Pakistan, Arabian Journal of Geosciences, (Accepted).
Kadri, I. B., 1991. Abnormal formation pressures in post-Eocene Formation, Potwar Basin, Pakistan. In: SPE/IADC drilling conference, 21920, Amsterdam, Netherland, March, 213-220(Abstract Book).
Karakan, C. O., 2009. Elastic and shear moduli of coal measure rocks derived from basic well logs using fractal statistics and radial basis function. Int. J. Rock Mech Min Sci, 46 (8): 1281-1295.
Khalid, P., Ahmed N., Yasin, Q., Ali, SH., 2012. Seismic Sequence Stratigraphy And Facies Analysis To Delineate The Reservoir Potential In Cretaceous -Tertiary Unconformity Of Middle Indus Basin, Punjab Platform, KSEG International Symposium on "Geophysics for Discovery and Exploration", 19-21(Abstract Book).
Khan, N., 2018. Comparative study of pore pressure in wells of Indus Offshore, southwest Pakistan. Arabian Journal for Science and Engineering, 43(1); 349-359.
Law, B. E., Shah, S. H. A., Malik, M. A., 1998. Abnormal high formation pressures, Potwar Plateau, Pakistan. AAPG Bull., 70: 247-258.
Law, B. E., Ulmishek, G.F., Slavin, V.I., 1994. Abnormal pressures in hydrocarbon environments. AAPG Memoir, 70: 1-11.
Leila, M., Sen, S., Abioui, M., Moscariello, A., 2021. Investigation of pore pressure, in-situ stress state and borehole stability in the West and South Al-Khilala hydrocarbon fields, Nile Delta, Egypt. Geomechanics and Geophysics for Geo-Energy and Geo-Resources, 7(3): 1-16.
Lisa, M., Khan, S. A., Khawaja, A. A., 2004. Focal Mechanism Studies of North Potwar Deformed Zone (NPDZ), Pakistan. ActaSeismologicaSinica, China, 17 (3): 255-261.
Malick, A. M., (1979). Pressures plague Pakistan's Potwar. In: Petroleum engineer, international, 20:26-36.
Meissner, C. R., Master, J .M., Rashid, M .A., Hussain, M., 1974. Stratigraphy of Kohat Quadrangle, Pakistan. United States Geological Survey. Reston, VA, USA; Professional Paper, 716-D.
Mouchet. J. P., Mitchell, A. F., 1989. Abnormal pressures while drilling: Origins, Prediction, Detection: Technical Manual, Elf Aquitaine Edition, 2: 225.
Mukerji, T., Dutta, N., Prasad, M., Dvorkin, J., 2002. Seismic detection and estimation of overpressures. Part I: The rock physics basis: CSEG Recorder, 27: 34-57.
Mukherjee, S., 2013. Channel flow extrusion model to constrain dynamic viscosity and Prandtl number of the Higher Himalayan Shear Zone. Int. J. Earth Sci, 102: 1811-1835.
Mukherjee, S., 2015. A review on out-of-sequence deformation in the Himalaya, Tectonics of the Himalaya. Geological Society, London, Special Publications, 412:67-109.
Nwonodi, R. I., Dosunmu, A., 2021. Analysis of a porosity-based pore pressure model derived from the effective vertical stress. Journal of Petroleum Science and Engineering, 204: 108727.
Opara, C., Adizua, O .F.,Ebeniro, J. O., 2018. Application of static correction in the processing of 3D seismic data from onshore Niger Delta. Universal Journal of Geoscience, 6: 1-7.
Paul, S., Chatterjee, R., Kundan, A., 2010. Determination of In-situ Stress Magnitudes for an Offshore Basin of Eastern India. 8th Biennial International Conference and Exposition on Petroleum Geophysics, Hyderabad, India, Feb. (Abstract Book, 151).
Radwan, A. E., Abudeif, A. M., Attia, M. M., Mohammed, M. A., 2019. Pore and fracture pressure modeling using direct and indirect methods in Badri Field, Gulf of Suez, Egypt. Journal of African Earth Sciences, 156:133-143.
Radwan, A. E., Abudeif, A. M., Attia, M. M., Elkhawaga, M. A., Abdelghany, W. K., Kasem, A. A., 2020. Geopressure evaluation using integrated basin modelling, well-logging and reservoir data analysis in the northern part of the Badri oil field, Gulf of Suez, Egypt. Journal of African Earth Sciences, 162: 103743.
Rana, R., Chandrashekhar, C., 2015. Pore pressure prediction a case study in Cambay basin. Geohorizons, 20 (1): 38.
Sahay, B., Fertl, W. H., 1988. Origin and evaluation of formation pressures. Kluwer Academic Publishers, Dordrecht, 10: 292.
Salim, A. M. A., Janjua, O. A., Wahid, A., Zaheer, A., 2015. Linear Regression Approach for Porosity and Permeability Calculations from Well Logs: A Case Study in NW Bonaparte Basin, Australia, 4th Annual International Conference on Geological & Earth Sciences (GEOS 2015), Singapore, (Abstract Book).
Sen, S., Kundan, A., Kumar, M., 2020. Modeling pore pressure, fracture pressure and collapse pressure gradients in offshore panna, western India: implications for drilling and wellbore stability. Natural

Resources Research, 29(4): 2717-2734.
Shah S.M.I., 2009. Stratigraphy of Pakistan: Memoirs of Geol. Surv. Pakistan, 22: 1-381.
Telford, W. M., Geldart, L. P., Sherrif, R. E., Keys, D. A., 2004. Applied Geophysics, 2nd Edition. Cambridge University Press, London, 760.
Terzaghi, K., 1943. Theoretical Soil Mechanics. Wiley, New York, USA.
Terzaghi, K., Peck, R. B., Mesri, G., 1996. Soil mechanics in engineering practice. John Wiley & Sons.
Thomas, E. C., Stieber, J. S., 1975. The Distribution of Shale in thrusting in terrestrial foreland basin; Application to the northwestern Himalaya, in Kleinspehn, K.L., and Paola, Cris, eds., New perspectives in basin analysis. New York, Springer-Verlag, 331-351.
Tingay, M. R., Hillis, R. R., Swarbrick, R. E., Morley, C. K., Damit, A. R., 2009. Origin of overpressure and pore-pressure prediction in the Baram province, Brunei. AAPG Bulletin, 93(1): 51-74.
Treloar, P. J., Coward, M. P., Williams, M. P., Khan, M. A., 1989. Basement-cover imbrication south of the Main Mantle thrust, north Pakistan. In: Malinconico, L. L. & Lillie, R. J. (eds) Tectonics of the western Himalayas. Geological Society of America, Special Paper, 275-294.
Velázquez-Cruz, D., Espinosa-Castañeda, G., Alberto, M., 2017. Determination of Pore Pressure Using Divergences, International Journal of Petroleum Science and Technology, 11(1): 51-63.
Wahid, A., Salim, A. M. A., Gaafar, G. R., Yusoff, A. W. I. W., 2016. Tectonic development of the Northwest Bonaparte Basin, Australia by using Digital Elevation Model (DEM), IOP Conference Series: Earth and Environmental Science, 30 (1):012005 (Abstract Book).
Wahid, A., Salim, A. M. A., Gaafar, G. R., Yusoff, W. I. W., 2016. The geostatistical approach for structural and stratigraphic framework analysis of offshore NW Bonaparte Basin, Australia. In AIP Conference Proceedings, 1705 (1): 020030. AIP Publishing LLC (Abstract Book).
Wandrey, C. J., Law, B. E., Shah, H.A., 2004. Patala-Nammal Composite Total Petroleum System, Kohat-Potwar Geologic Province, Pakistan. US Geological Survey, 1-18.
Wang, Z., Wang, R., 2015. Pore pressure prediction using geophysical methods in carbonate reservoirs: Current status, challenges and way ahead. J. Nat. Gas Sci. Eng., 27: 986-993.
Wasim, P., 2004. Kohat Plateau with Reference to Himalayan Tectonic General Study, Canadian Journal of Exploration Geophysics, 29:04.
Wyllie, M. R. J., Gregory, A. R., Gardner, G.H.F., 1958. An experimental investigation of the factors affecting elastic wave velocities in porous media. Geophysics, 23: 459-493.
Yasin, Q., Baklouti, S., Khalid, P., Ali, S. H., Boateng, C. D., Du, Q., 2021. Evaluation of shale gas reservoirs in complex structural enclosures: A case study from Patala Formation in the Kohat-Potwar Plateau, Pakistan. Journal of Petroleum Science and Engineering, 198: 108225.
Yu, H., Wang, Z., Rezaee, R., Zhang, Y., Han, T., Arif, M., Johnson, L., 2018. Porosity estimation in kerogen-bearing shale gas reservoirs. Journal of Natural Gas Science and Engineering, 52:575-581.
Zaidi, S. N. A., Brohi, I. A., Ramzan, K., Ahmed, N., Mehmood, F., Brohi, A. U., 2013. Distribution and hydrocarbon potential of Datta sands in Upper Indus Basin, Pakistan. Sindh University Research Journal-SURJ (Science Series), 45(2).
Zeitler, P. K., Tahirkheli, R. A. K., Naesser, C., Johnson N., Lyons J., (1981). Preliminary fission track ages from the Swat Valley, northern Pakistan. Geological Bulletin of the University of Peshawar, 180-182.
Zhang, J., 2011. Pore pressure prediction from well logs: methods, modifications, and new approaches. Earth-Sci. Rev, 108:50-63.
Zhang, J., 2013. Effective stress, porosity, velocity and abnormal pore pressure prediction accounting for compaction disequilibrium and unloading. Marine and Petroleum Geology, 45: 2-11.
Zhang, J., Zheng, H., Wang, G., Liu, Z., Qi, Y., Huang, Z., Fan, X., 2020. In-situ stresses, abnormal pore pressures and their impacts on the Triassic Xujiahe reservoirs in tectonically active western Sichuan basin. Marine and Petroleum Geology, 122:104708.
Zhang, Q., Choo, J., Borja, R. I., 2019. On the preferential flow patterns induced by transverse isotropy and non-Darcy flow in double porosity media. Computer Methods in Applied Mechanics and Engineering, 353:570-592.